ISSN 0169-6548

Communications on hydraulic and geotechnical engineering

Analysis of the transport of a pollution cloud in the Upper-Rhine River between Lake of Constance and Basel

May 1994

C.A. van Kuik / A. van Mazijk

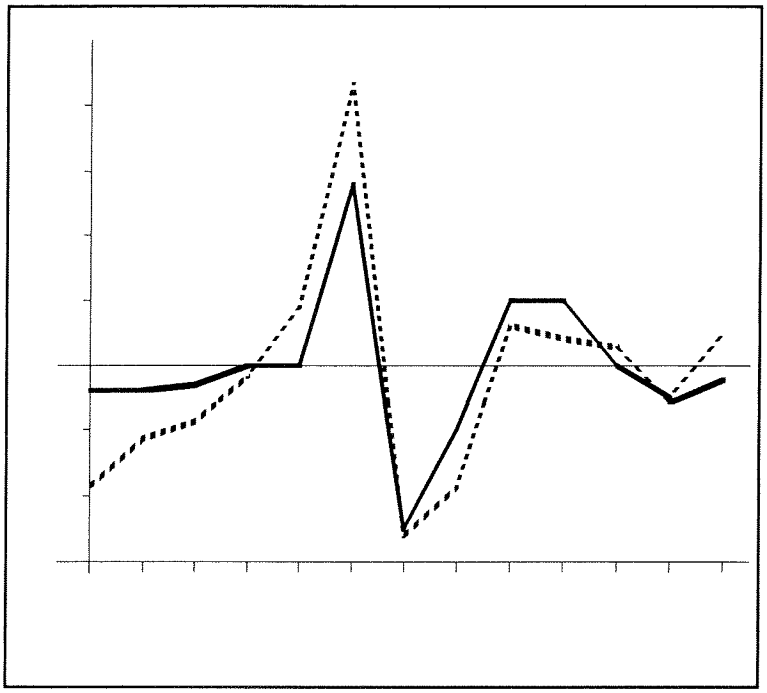

TUDelft
Delft University of Technology

Faculty of Civil Engineering

Analysis of the transport of a pollution cloud in the Upper-Rhine River between Lake of Constance and Basel

by

C.A. van Kuik

and

A. van Mazijk

May 1994

Communications on Hydraulic and Geotechnical Engineering

Report No. 94 - 4

Faculty of Civil Engineering

Delft University of Technology

Abstract

In the one-dimensional 'Rhine Alarm Model' differences between the actual travel time of a pollution cloud, originating from an instantaneous release of an accidental spill, and the travel time, based on the flow velocity is represented by a *lag* coefficient. In the model this *lag* coefficient is defined by the relative difference between these two travel times.

This paper presents the results of a study on the influence of tributaries and suppressed flow by weirs on the *lag* coefficient in general and on the influence of the River Aare and the suppressed flow by water power stations on this coefficient in the Upper-Rhine River between Lake of Constance and Basel especially. Also the influence of incompletely transversal mixing in the vicinity of the point of release at a river bank as a special case of a polluted tributary is discussed.
In the study analytical and numerical approaches were applied. For the numerical approach a two-dimensional transport model of the "Versuchsanstalt für Wasserbau (VAW)" (Hydraulic Research Institute) of the ETH-Zürich (Federal University of Technology of Zürich) was used.

The main conclusion is that the behaviour of the *lag* coefficient along the Upper-Rhine River is strongly influenced by sudden increases of the flow velocity at power stations, due to the differences in waterdepth upstream and downstream of the station, and at the Aare-Rhine confluence, due to the large discharge ratio of these river branches. The outcome of these flow-velocity discontinuities is a relatively large negative value of the *lag* coefficient upstream of the discontinuity and a relatively large positive value downstream. This is because upstream of the discontinuity the transport velocity of the centroid of the pollution cloud is already influenced by the larger flow velocity downstream of the discontinuity as soon as the front of the cloud has passed the discontinuity. Downstream of the discontinuity the transport velocity of the centroid is still influenced by the smaller flow velocity upstream of the discontinuity as long as the tail of the cloud remains upstream of the discontinuity.

Case studies on the Upper-Rhine River between Lake of Constance and Basel show good fits of the calibrated values of the *lag* coefficient in the Rhine Alarm Model with the results of the two-dimensional transport model.

Acknowledgment

Prof. dr. M. de Vries is gratefully acknowledged for his encouraging support and critical reading of this report.

Table of contents

Chapter 1

Introduction

The Rhine Alarm Model uses the modified Taylor Model in which the travel times of substances are calculated in relation to the travel times of the water particles (Spreafico and van Mazijk, 1993). The time lag of the substance compared with the water particles is defined by a *lag* coefficient after Eq.(1)

$$\beta = \frac{u_s}{c} - 1 = \frac{T_{pol}}{T_{flow}} - 1 \qquad (1)$$

wherein u_s and c are the velocities of the flow and the pollution cloud respectively and T_{flow} and T_{pol} the respective travel times.
These lag coefficients are calibrated for the Swiss reach of the River Rhine between Rheinau and Basel (van Mazijk, 1992) and showed in Fig. 1.

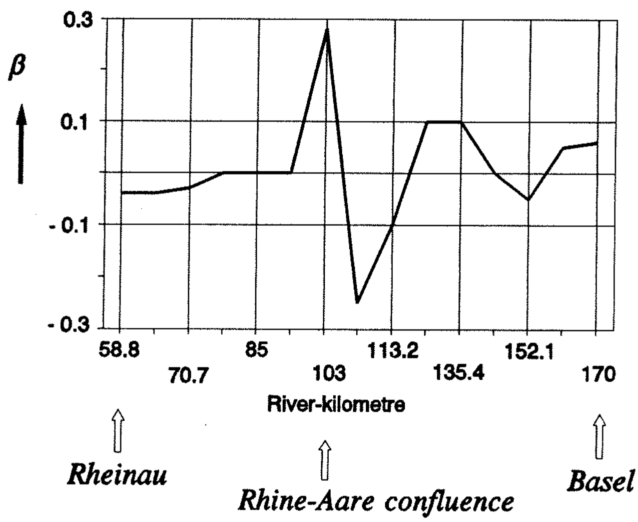

Fig. 1. Distribution of the calibrated lag-coefficient β along the Swiss reach of the River Rhine between Rheinau and Basel.

The lag coefficient β in the vicinity of the river confluence AARE-RHINE (at 103 km) shows a positive value (0.28) upstream of the confluence, and a negative value (-0.25) 8 km downstream. Van Mazijk (1992) concluded, that this behaviour must be the outcome of two-dimensional effects caused by the flow at the confluence.

The verification of this conclusion is the main reason for the analysis of the behaviour of the lag coefficient β at a river confluence as well as in the near-field of a point release, which can be considered as a special case of a river confluence with a very small polluted branch.

The study has been split into two different approaches:
* Analytical analysis, based on analytical solutions for the 2-D convection-diffusion equation.
* Numerical analysis. Analysis with the use of a two-dimensional transport model of the "Versuchsanstalt für Wasserbau (VAW)" (Hydraulic Research Institute) of the ETH-Zürich (Federal University of Technology of Zürich).

In this paper these different approaches will be explained as well as the assumptions applied. After this description the numerical calculations for an *idealized* river will be discussed and compared with the analytical analysis. The *idealized* river is characterized by a constant cross-section and a constant discharge. In case of a tributary the discharge and the cross section only can change at the confluence.

In the last part numerical calculations for some case-studies of the Upper-Rhine River are carried out and the most important influences on the β-coefficient are presented. In the final part of this paper the resulting β-coefficients of these case-studies are compared with the calibrated coefficients in the 'Rhine Alarm Model'.

Chapter 2

Analytical approach

2.1 GENERAL

For the analytical approach of the two-dimensional aspects in transport phenomena of a substance two situations are considered:

* a continuous point release at a river bank;
* a river confluence.

For the analysis of the behaviour of the lag-coefficient β, an analytical description of the concentration distribution in the two horizontal directions x and y is necessary.

2.2 CONCENTRATION ANALYSIS

2.2.1 Release at a river bank

In case of a release of a substance at the river bank three mixing phases can be distinguished (see Fig. 2):

1. a first phase in which vertical mixing is predominant;
2. the second phase in which transversal mixing over the cross-sectional area of the river is predominant and
3. the third phase in which longitudinal mixing is predominant for the distribution of the concentration of the released substance.

In rivers with a large width/depth ratio (more than 20) the distance over which vertical mixing has become complete, is still relative short (about 60 to 100 times the waterdepth). In such situation the two-dimensional convection-dispersion equation gives a reasonable description of the transport phenomena. Considering a constant release of a conservative substance W the analytical solution for the concentration distribution $\varphi(x,y)$ becomes

$$\frac{\varphi(x,y)}{\varphi_0} = \frac{1}{\sqrt{(\pi K_y x)/(u_s \cdot B_s^2)}} \cdot \sum_{n=-\infty}^{n=\infty} \left(\exp\left(- \frac{(y/B_s - 2n)^2}{(4K_y x)/(u_s \cdot B_s^2)} \right) \right) \qquad (2)$$

with

φ_0 average cross-sectional concentration (W/A)
A cross-sectional area of the river
K_y transversal dispersion coefficient
B_s width of the river
u_s average cross-sectional velocity
x x-coordinate along the river
y y-coordinate along the transverse direction

Defining a completely mixed situation over the cross-sectional area of the river by $\varphi/\varphi_0 \geq 0.95$ it can be derived from Eq.(2) that this will be achieved at a distance L_m

$$L_m = 0.4 \frac{u_s \cdot B_s^2}{K_y} \tag{3}$$

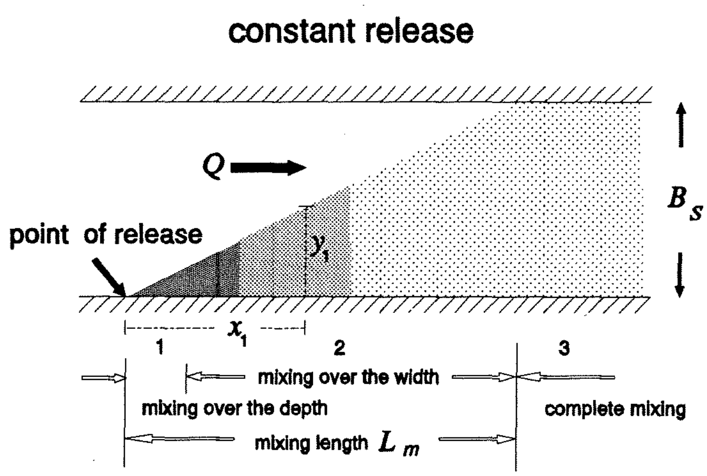

Fig. 2. The three mixing phases.

2.2.2 River confluence

In case of a river confluence also the mixing zone over the width (second phase) is important, see Fig. 3.
When upstream the concentration in the polluted river has reached an equilibrium (Noppeney, 1988) the conditions at the begin of the confluence are defined by

$$\varphi(0,y) = 0 \qquad \text{if } y/B_s > B_1/B_s$$
$$\varphi(0,y) = (B_s/B_1)*W/Q \qquad \text{if } y/B_s < B_1/B_s$$

The final solution of the concentration distribution downstream the river confluence is given by

$$\frac{\varphi\ (x',y')}{\varphi_0} = \frac{B_s}{2B_1}\left[\sum_{n=-\infty}^{\infty} \text{erf}\left(\frac{y'-2n+\frac{B_1}{B_s}}{2\sqrt{x'}}\right) - \sum_{n=-\infty}^{\infty} \text{erf}\left(\frac{y'-2n-\frac{B_1}{B_s}}{2\sqrt{x'}}\right)\right] \tag{4}$$

with

$$x' = \frac{x \cdot K_y}{u_s \cdot B_s^2} \qquad y' = \frac{y}{B_s} \tag{5}$$

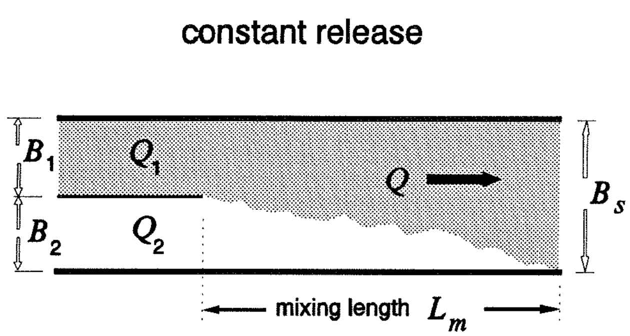

Fig. 3. Mixing at a confluence starting with a width ratio B_1/B_s.

2.3 LAG-COEFFICIENT ANALYSIS

2.3.1 General

This analysis consists of two different methods.

The first is called the '*linear spreading method*'. This method assumes a linear increase of the 'spreading width' of the pollutant with the distance from the point of release (Fig. 2). The distance of the completely mixed situation over the whole cross-sectional area of the river is given by Eq.(3). Over the 'spreading width' a completely mixed situation is assumed (Fig. 5).

The second one is called the *'flux method'*. This method assumes a specific concentration profile over the width depending of the distance from the point of release after Eq.(2).

For the analysis of the lag coefficient in both cases the same exponential velocity profile is used, with a variable n after Eq.(6).

It yields for $y \leq 0.5\ B_s$

$$u(y) = \frac{n+1}{n} \cdot \left(\frac{y}{0.5\ B_s}\right)^{\frac{1}{n}} \cdot u_s \tag{6}$$

and for $0.5\ B_s < y < B_s$

$$u(y) = \frac{n+1}{n} \cdot \left(\frac{B_s - y}{0.5\ B_s}\right)^{\frac{1}{n}} \cdot u_s \tag{7}$$

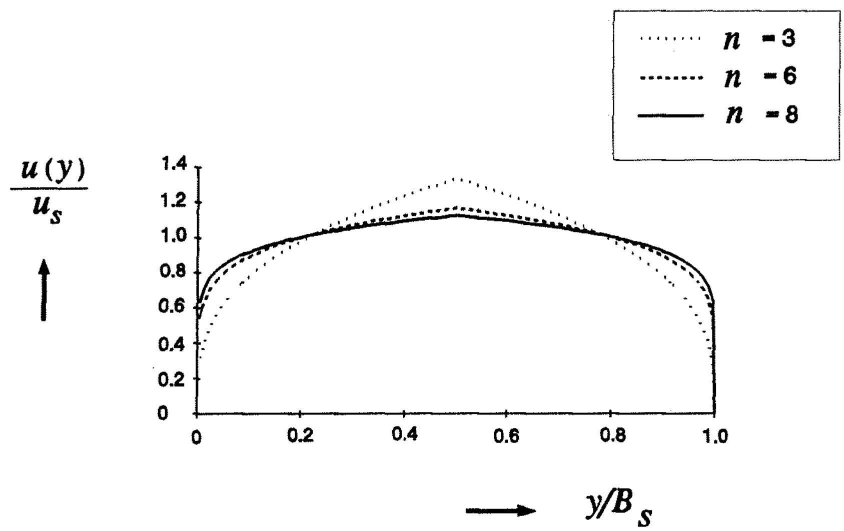

Fig. 4. Exponential velocity profile.

2.3.2 Linear spreading method

In case of the linear increase of the 'spreading width' with the distance (see Fig. 2) the transport velocity $c(x_1)$ at a certain distance x_1 is assuming to be equal the mean velocity over the spreading width y_1 defined by (see also Appendix)

$$c(x_1) = \overline{u(y_1)} = \frac{1}{y_1}\int_0^{y_1} u(y)\mathrm{d}y \tag{8}$$

with

$$y_1 = \frac{x_1}{L_m} \cdot B_s \tag{9}$$

Substitution of Eqs (6) and (9) into Eq.(8) the integration of Eq.(8), applying the dimensionless distance $X_1 = x_1/L_m$ gives for $X_1 \leq 0.5$

$$c(X_1) = \left(2 \cdot X_1\right)^{\frac{1}{n}} \cdot u_s \tag{10}$$

In a similar way the transport velocity for values of $X_1 > 0.5$ can be derived

$$c(X_1) = \frac{1}{X_1} \cdot \left[1 - 2^{\frac{1}{n}} \cdot \left(1 - X_1\right)^{\frac{n+1}{n}}\right] \cdot u_s \tag{11}$$

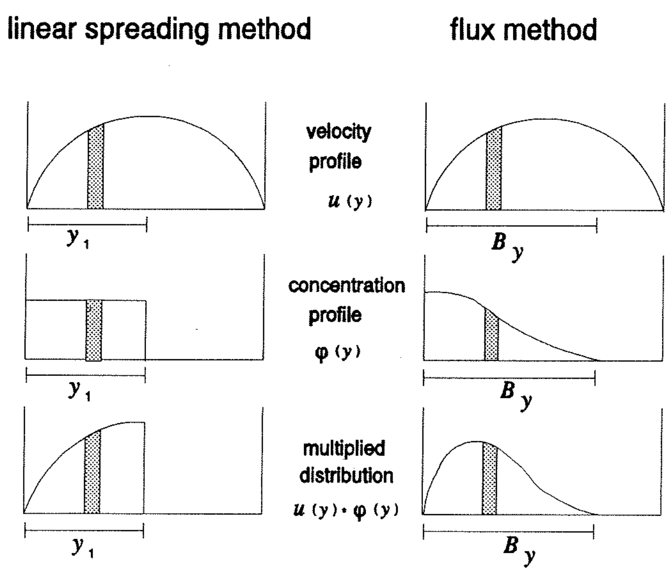

Fig. 5. The two different analytical methods.

Applying Eq.(1) the local lag coefficient can be computed from Eqs (10) and (11), being a local value at a distance X_1 from the point of release. The overall value of the coefficient at this distance is found by integrating the local lag coefficient over this distance and dividing by the same distance from the point of release (see Appendix).

It yields for $X_1 < 0.5$

$$\overline{\beta(X_1)} = \frac{1}{X_1} \int_0^{X_1} \left[(2 \cdot X)^{-\frac{1}{n}} - 1 \right] dX \tag{12}$$

and for $0.5 < X_1 < 1$

$$\overline{\beta(X_1)} = \frac{1}{X_1} \int_0^{0.5} \left[(2 \cdot X)^{-1/n} - 1 \right] dX + \frac{1}{X_1} \int_{0.5}^{X_1} \left[\frac{X}{1 - 2^{1/n}(1 - X)^{(n+1)/n}} - 1 \right] dX \tag{13}$$

2.3.3 Flux method

In case of a release at the riverbank the concentration distribution is defined by Eq.(2) and in case of a river confluence by Eq.(4).
Using these concentration distributions and the exponential velocity-distribution after Eqs (6) and (7) the flux method consists of five steps:

1. The multiplication of the two distributions for every y-value of the cross-section (see Fig. 5).

2. The integration of this multiplication over the width of the river defined as the flux of the pollutant, $F(x)$ for each cross-section, see Eq.(14).

$$F(x) = \int_0^{B_s} \left(u(y) \cdot \frac{\varphi(x,y)}{\varphi_0} \right) dy \tag{14}$$

3. Determining the mean velocity of the pollution cloud $c(x)$ with Eq.(15).

$$c(x) = \frac{F(x)}{B_y} \tag{15}$$

wherein B_y is the partial width of the river over which the pollutant has been spread ($\varphi(x,y)/\varphi_0 \geq 0.01$, see Fig. 5).

4. Defining the local lag coefficient after Eq.(1) concerning the local mean velocity of the flow and the pollutant

$$\beta(x) = \frac{u_s(x)}{c(x)} - 1 \tag{16}$$

5. Defining the overall lag coefficient by integration of the local lag coefficient in the main flow direction from the point of release in the same way as explained for the 'linear spreading method'.

These calculation steps are executed with a numerical program, because no analytical solution as for the 'linear spreading method' can be derived.

Chapter 3

Programs for the numerical analysis

3.1 GENERAL

The numerical analysis is carried out with the hydrodynamic model FLORIS and the transport model PORIS of the Hydraulic Research Institute VAW (Versuchsanstalt für Wasserbau, Wasserwirtschaft und Glaziologie) of the ETH-Zürich (Federal University of Technology of Zürich) and the program BETA all written in the FORTRAN-language. The two models of the VAW decribe the flow and pollutant conditions. The program BETA translates the results of these models into vaules for the lag coefficient.

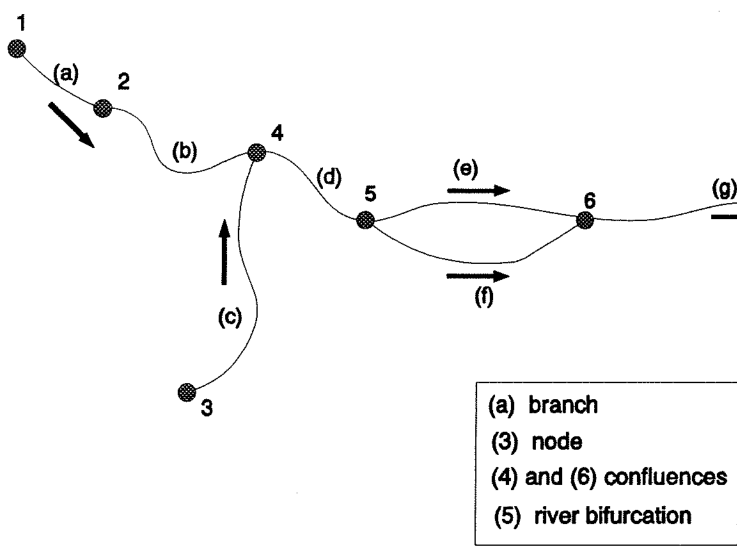

Fig. 6. FLORIS basic structure scheme.

3.2 PROGRAM FLORIS

FLORIS is an one-dimensional hydrodynamic flow model based on the Saint-Venant equations (VAW, 1991). In the model the river is schematized in branches and nodes (Fig.6). This schematisation is also suitable for river confluences. The program consists of two input files:

1. **FUNIN** file. This file registers the distinguished cross-sectional profiles of the river. Each cross section is characterised by a name, the x-coordinate, the bed level along the y-coordinate, the roughness etc.

2. **FLOIN** file. This file registers the branches, nodes and their connection to each other. Each branch is characterised by a name, the number of the downstream and upstream node, bottom slope, etc.

Each node can be characterised by

* boundary conditions

$Q_{hydrograph}$	time related discharge.
Water level	used at river confluences.
Water-level regulation	by a weir, etc.
* $Q_{lateral}$	in- or outflow of water at a cross-section (tributary, bifurcation) or uniformly distributed along a branch (ground water inflow or withdraw).

3.3 PROGRAM PORIS

This program is based on the streamtube approach for the calculation of the transport of a substance in terms of concentration distributions per streamtube, (VAW, Dec. 1991) and uses the output of the mean flow velocity computed by FLORIS. For the expansion of the pollutant in each streamtube there are two processes taken into account by the program PORIS:

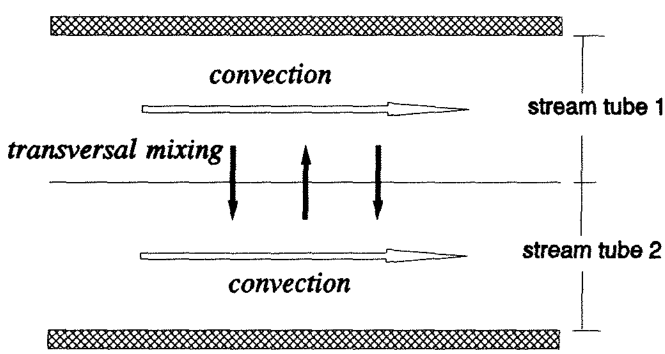

Fig. 7. Processes of PORIS.

* The convection in a stream tube. Due to the different velocities in each tubes, the process of longitudinal dispersion is simulated. Theoretically this is not totally correct, but it is a realistic approximation.
* The transverse mixing between the each stream tube. This process is described by the transverse mixing coefficient

$$K_y = \alpha \cdot u_* \cdot a \qquad (17)$$

with
α constant of proportionality
a water depth
u_* shear velocity

3.4 PROGRAM BETA

With the program BETA the lag coefficients are calculated, using the numerical output of the programs FLORIS and PORIS. The results are presented graphically. In the program BETA there are two different approaches to be distinguished for the determination of the lag coefficient:

The first approach concerns the '*overall*' lag-coefficient (see Eq.(18)) as a integrated value from the point of release to the cross-section concerned ($cross_m$). Thus in Eq.(18) T_{pol} and T_{flow} are the respective travel-times of the pollutant and the flow integrated over the distance from the point of release to the cross-section concerned.

$$\beta = \frac{T_{pol_{cross_m}}}{T_{flow_{cross_m}}} - 1 \qquad (18)$$

The second approach concerns the '*local*' lag-coefficient, which reveals the detailed information of the differences between the travel time of the flow in comparison with the travel time of the pollutant between two adjacent cross-sections. The local coefficient is defined by

$$\beta_m = \frac{T_{pol_{cross_{m+1}}} - T_{pol_{cross_m}}}{T_{flow_{cross_{m+1}}} - T_{flow_{cross_m}}} - 1 \qquad (19)$$

The program FLORIS is used for the calculation of the travel times of the flow.
The output of FLORIS consists of flow velocity values at the different cross sections.

Integration of these velocities, with the assumption of a constant flow velocity between two adjacent cross-section yields the travel times of the flow

$$T_{flow} = \frac{(x_{cross_{m+1}} - x_{cross_m})}{u_{cross_m}} \tag{20}$$

The program PORIS is used for the computation of the travel time of the pollution cloud. The output of PORIS consists of concentration distributions in the space domain per time step and per stream tube. Integration of the concentrations in x- and y-direction yields for each time step the total mass m_0 (i.e. 0^{th} moment of the concentration distribution) after Eq.(21)

$$m_0 = \int_0^{x_{fr}} \int_0^{B_s} \varphi(x,y)\, dy\, dx \tag{21}$$

with x_{fr} as the distance from the point of release to the cross section directly ahead of the pollution cloud.

The position of the centroid of the pollution cloud in the space domain (μ_x) at a certain time is computed with the help of the first moment m_1 of the concentration distribution (Eq.(22)).

$$\mu_x = \frac{m_1}{m_o} = \frac{1}{m_o} \int_0^{x_1} \int_0^{B_s} (x - x_{inlet}) \cdot \varphi(x,y) dx dy \tag{22}$$

Assuming no significant transformations of the concentration distribution during the passage of the pollution cloud at a certain cross section ("frozen cloud approach") the travel time of the centroid can be determined from the computed x-coordinates (μ_x) with the corresponding time steps. With the travel times of the flow the '*overall*'-delay coefficient is can be determined by Eq.(18) and the '*local*' coefficient by Eq.(19).

Chapter 4

Numerical analysis of an idealized river

4.1 GENERAL

An *idealized* river is characterized by a constant cross-section and a constant discharge. In case of a tributary the discharge and the cross section only can change at the confluence.

The topography of the river used for the analysis is shown in Fig. 8.

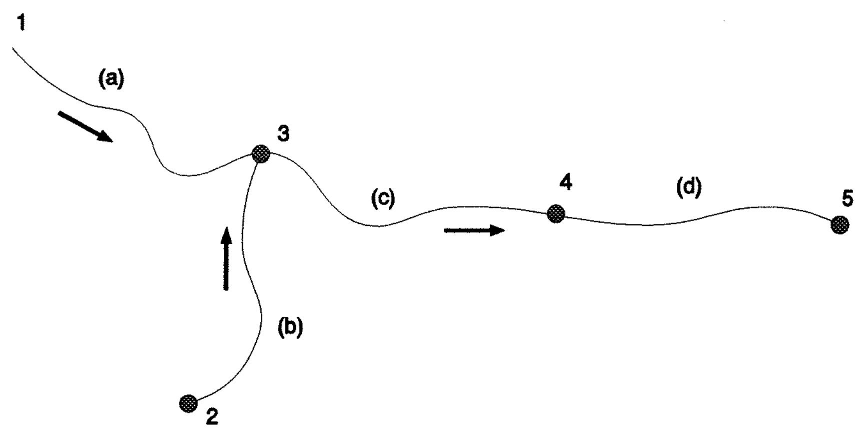

Fig. 8. Structure scheme for an idealized river.

For the investigation of the lag coefficient various characteristics of the flow and pollutant conditions are considered, representing all kinds of influences on the local lag-coefficient.

The most important characteristics of the reference case-study are:
* river width (B_s) 200 m
* discharge (Q) 1000 m^3/s
* constant of proportionality (α) after Eq.(17) 0.23

For the velocity profile in the cross section the exponential one after Eq.(6) is considered with $n = 8$ (see also Fig. 4).

Three situations are investigated:
(1) near-field aspects for an instantaneous point release,
(2) river confluence and
(3) water-level regulation by weirs in connection with power stations.

4.2 NEAR-FIELD

In case of near-field effects on the value of the lag coefficient the following parameters are examened:
* the location of the point of release in the cross-section of the river
* discharges of the river
* constant of proportionality α, concerning the transverse mixing

Location of the point of release
After the velocity profile decribed by Eq.(6) the transport velocity of the pollutant is smaller than the mean flow-velocity if the point of release is located at the river bank. As a result, the lag coefficient is positive. If the location is in the middle of the river the lag coefficient becomes negative. (see Fig. 9)

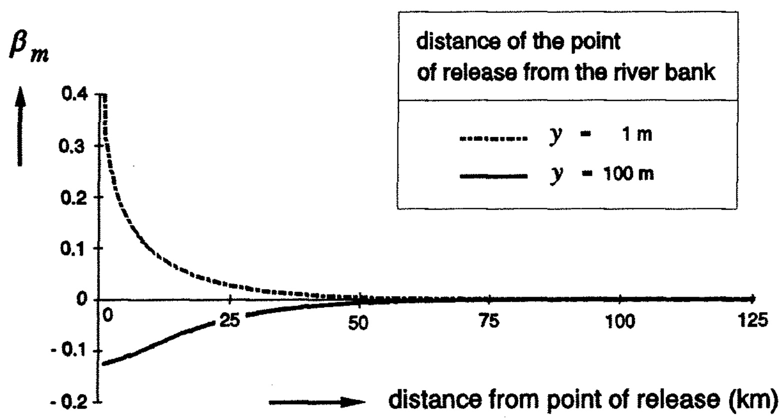

Fig. 9. Lag coefficients with different locations of release from the river bank (river width = 200 m).

River discharge
An increment of the discharge implies more transversal mixing caused by the shear-velocity u_* (see Eq.(17)). As a result the distance over which the local delay-coefficient becomes zero decreases (Fig. 10).

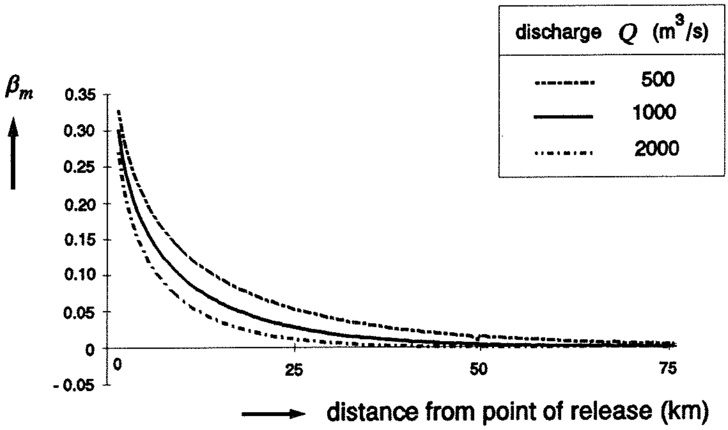

Fig. 10. Distribution of the local lag-coefficient β_m for different river-discharges.

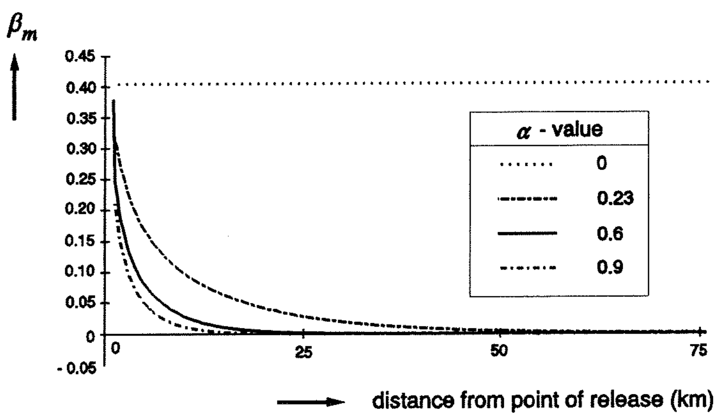

Fig. 11. Distribution of the local lag-coefficient β_m for different α-values.

Constant of proportionality for the transverse mixing
Increasing the constant α means after Eq.(17) an increase of the transverse mixing with the same rate. This increase has the same influence on the lag coefficient as the an increase of the river discharge (see above). If the mixing coefficient is zero, then the pollution cloud remains in the stream tube where the inlet is situated. The local lag-coefficients are constant, while the travel-time difference between the flow and the pollution cloud does not change (Fig. 11).

4.3 RIVER CONFLUENCE

4.3.1 General

In this study a confluence is located 50 km downstream from a point release at the river bank.
Regarding the confluence, two aspects influence the lag coefficient:
* The turn-over process, caused by a *discontinuity of the flow velocity* upstream and downstream of the confluence (in case of an one-dimensional approach)
* The *discontinuity of the width* over which the pollutant is spread upstream and downstream of the confluence. Upstream of the confluence the pollutant is completely mixed over the width of the river branch concerned. Immediately downstream of the confluence the pollutant is spread over a certain width, related to the width ratio of the concerned branches upstream and downstream of the confluence (Fig. 3).

4.3.2 Discontinuity of the flow velocity

When a pollution cloud meets a river confluence three situations can be distinguished (see Fig. 12):

(a) The centroid of the pollution cloud is located *upstream of the confluence*. Depending on the number of cross-sections over which the pollution cloud is spread a part of the cloud has already entered the larger velocity downstream of the confluence, thus the velocity of the centroid of the pollution cloud c is increasing. Because the centroid is still located upstream of the confluence, the velocity c is related to the smaller flow-velocity u_s in this river branch. This means that after Eq.(1) the lag-coefficient β related to the centroid becomes negative (see also Fig. 15).

(b) When the centroid is just located at the river confluence, one part of the cloud is in the slower and one part in the faster zone of velocity, thus $d\beta/dx$ becomes infinite.

(c) The opposite situation takes place for the downstream branch of the river-confluence section.
The pollution cloud is slower, while one part of the cloud is still situated upstream. Thus the lag-coefficient β becomes positive.

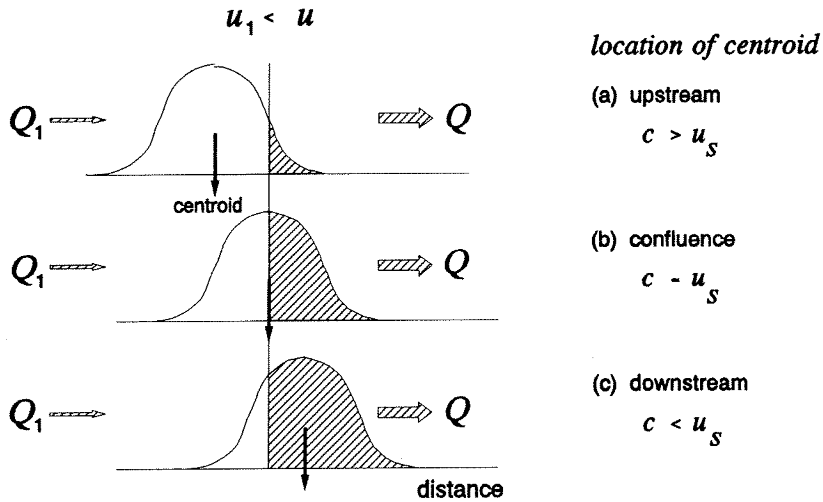

Fig. 12. Behaviour of the pollution cloud at a confluence (see Fig. 3).

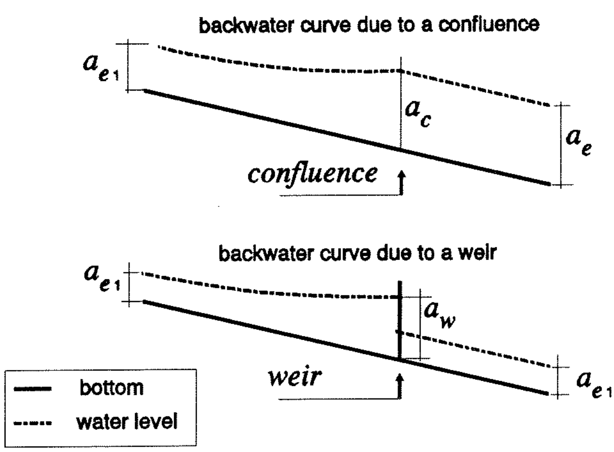

Fig. 13. Water-level profile at a river confluence and a weir.

This process is called the *turn-over process*. The result of this process is the sudden change of the lag coefficient with upstream a negative peak and downstream a positive one. This effect is unavoidable for all cases where the flow velocities show a discontinuity (Fig.15). The small positive values of the lag coefficient upstream of the large negative peak is caused by a certain reduction of the transport velocity c as a result of the backwater upstream of the confluence (see Fig. 13) in case of a relative large inflow of the non-polluted branch. In this situation the pollution cloud is located completely upstream of the confluence, while at the position of the centroid of the cloud the backwater has still a negligible effect on the flow velocity.

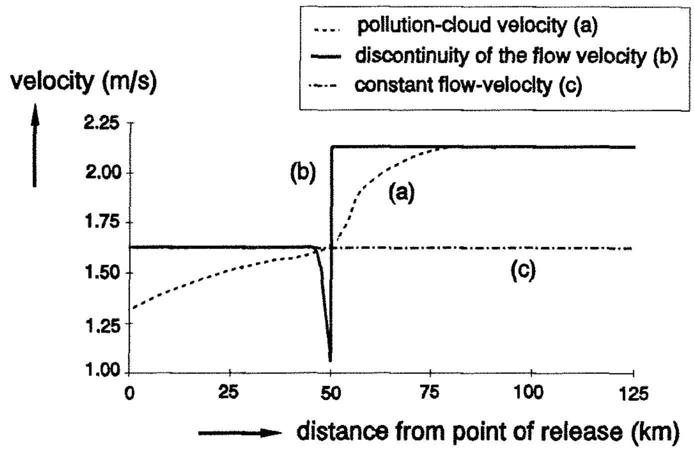

Fig. 14. Longitudinal distribution of the flow and pollution-cloud velocity at a confluence.

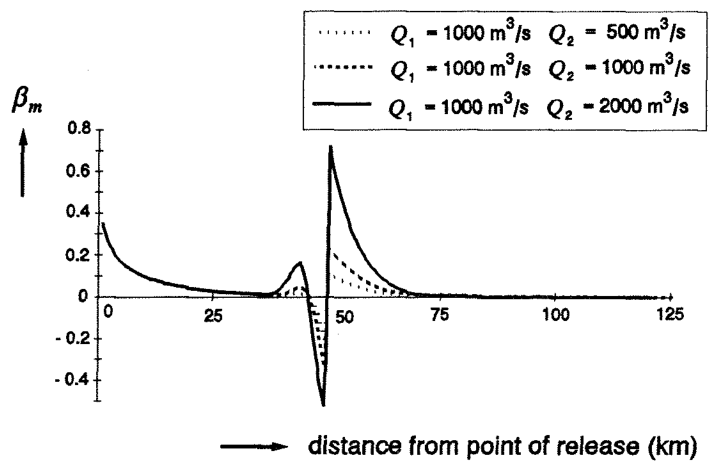

Fig. 15. Lag coefficients with different discharge-ratios of the upstream river branches of a confluence.

The effect of the discharge (Q_2) of the non-polluted branch on the local value of the lag coefficient shows to be proportional (Fig. 15).

4.3.3 Discontinuity of the river width

In this sub-section only a discontinuity in the river width as a result of the confluence is concerned. In this study the width of the polluted river-branch B_1 is varied, keeping the total width of the river downstream of the confluence (B_s) constant. It yields (see also Fig. 3)

$$B_s = B_1 + B_2 \tag{23}$$

In the applied two-dimensional transport model the ratio of the width of the polluted branch (B_1) and the total width (B_s) is related to the discharges respectively after Eq.(24).

$$\frac{B_1}{B_s} = \frac{Q_1}{Q} \tag{24}$$

with $Q = Q_1 + Q_2$ (see Fig. 3).

Therefore the variation of the width B_1 was achieved by varying the total discharge Q and keeping the discharge of the polluted river branch (Q_1) constant as well as the total width (B_s).
In this way the mean flow-velocity does not change at the confluence (see case (c) of Fig. 14).

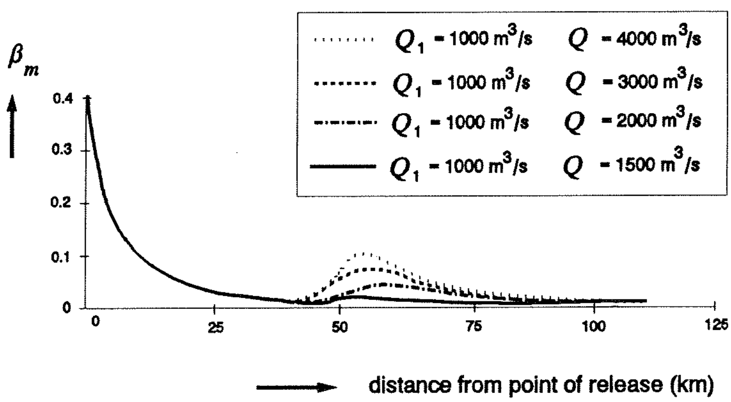

Fig. 16. Distribution of the lag coefficient for several discharge ratios i.e. width ratios at a confluence.

In Fig. 16 the influence of the variation of the width of the non-polluted branch of the confluence, i.e. the variation of the discharge ratio Q_1/Q on the lag coefficient is presented. As expected the lag coefficient is positive downstream of the confluence and comparable with the situation of a point release at a river bank, i.e. a polluted river branch with a width equal zero.

4.4 WATER-LEVEL REGULATION BY A WEIR

This case-study concerns the regulation of the water level with a fixed water depth a_w upstream of the weir of 8 m. The equilibrium water-depth a_e is 2.9 m with a mean flow-velocity of 1.62 m/s (Fig. 13). The weir is located 50 km downstream of the point of release.

As a result of the discontinuity in water depth upstream and downstream of the weir there is a discontinuity in the mean flow-velocity over the weir. This means that the influence of the weir on the lag coefficient must be similar to the influence of a relative large inflow of a tributary at a confluence, which also results in a discontinuity of the mean flow-velocity as discussed in Section 4.2.

This similarity is confirmed by the calculated distribution of the local lag-coefficient presented in Fig. 17.

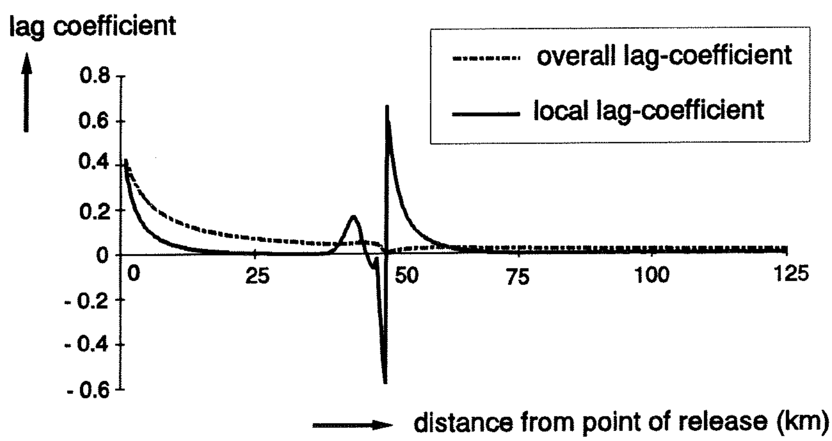

Fig. 17. Distribution of the lag coefficient in case of a water-level regulation by a weir.

Chapter 5

Comparison between the analytical and numerical calculations

5.1 GENERAL

For the comparison of the analytical calculations with the numerical one the reference case- study of the idealized river will be used (see Chapter 4). For the comparison two situations are considered:
(a) a point release at the river bank and
(b) a river confluence.

Another important parameter for the comparison between the numerical and analytical results is the n-value of the applied velocity-profile (see Eq.(6)). All numerical calculations are executed with $n = 8$. In case of the analytical approaches different n-values are applied.
In case of a point release the two analytical approaches (*linear spreading method* and *flux method*) are considered. For the river confluence only the *flux method* is discussed.

5.2 LINEAR SPREADING METHOD FOR A POINT RELEASE AT A RIVER BANK

In case of the linear spreading method the mixing length L_m (see Eq.(9)) has to be known. For the determination of this length there are two approaches:
* An analytical one based on Eq.(3) and
* A numerical one based on calculations of the lag coefficient with the program BETA. In this approach the mixing length is the distance over which the local lag-coefficient diminish to zero.

Using the numerical approach for the reference case-study a mixing length of 70 km is found. Figure 18 shows the results. The distribution of the overall lag-coefficient in case of the numerical approach with $n = 8$ is similar to the analytical output for $n = 12$, but differs from the analytical output for $n = 8$.

However, the value $n = 12$ is not a common one for natural streams. The reason for the similarity is the difference in the transversal spreading of the pollutant between the the numerical and analytical approach. As a matter of fact the transversal spreading is larger in the case of the numerical approach, according to the two-dimensional description of the transport of a substance after Eq.(2) than in case of the analytical method, assuming a linear spreading with the distance from the point of release (see also Fig. 20). Therefore the large value for n in the analytical approach is needed to compensate this difference in transversal mixing (see also Section 5.3).

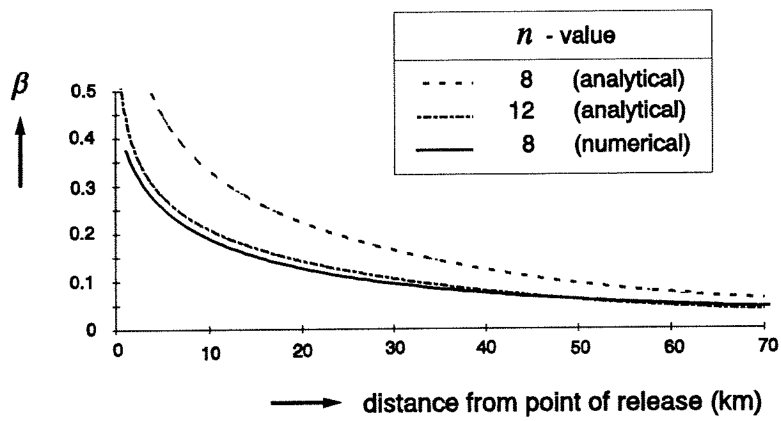

Fig. 18. Verification *lineair spreading method.*

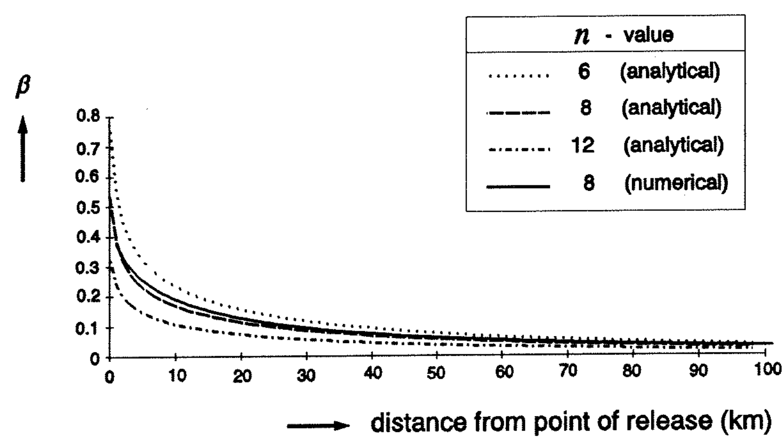

Fig. 19. Verification *flux method* with $\alpha = 0.23$.

5.3 FLUX METHOD FOR A POINT RELEASE AT A RIVER BANK

Using the flux method the results of the numerical calculations with $n = 8$ correspond quite well with the analytical one for $n = 8$ (Fig. 19). This similarity between the analytical and numerical approach can be qualified as an advantage of the *flux method* against the *linear spreading method.*

Another advantage of the *flux method* concerns the mixing length. In the *linear spreading method* the mixing length has to be determined previously, while in the *flux method* the mixing length is determined automatically.

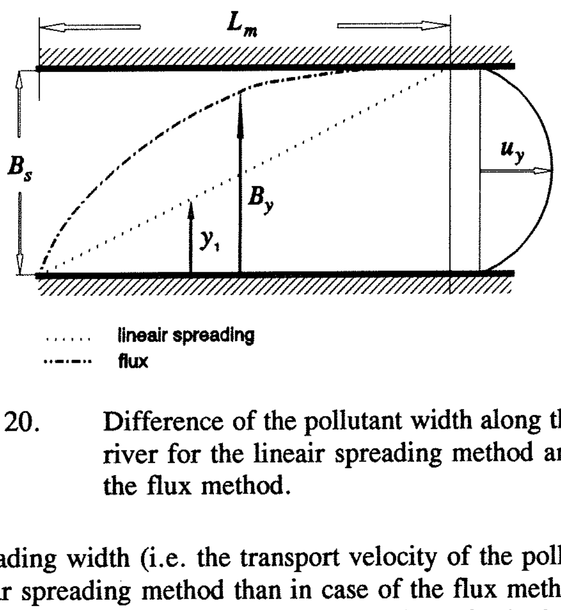

Fig. 20. Difference of the pollutant width along the river for the lineair spreading method and the flux method.

The reason for the agreement of the results of the *flux method* and the *numerical approach* with $n = 8$ is as follows. Near the point of release the pollutant is spread actually over a larger part of the river width as assumed by the *linear spreading method* (see Fig. 20), whereas the *flux method* describes the transversal spreading correctly.

This means that at a certain location the mean flow velocity over the spreading width (i.e. the transport velocity of the pollutant) is smaller in case of the linear spreading method than in case of the flux method, using the same n-value. In other words to get the same lag coefficients for both methods the n-value has to be chosen larger in case of the linear spreading method than in case of the flux method. Therefore the n-value of 12 in case of the linear spreading method gives a good agreement of the distribution of the lag coefficient with the distribution found by the numerical approach with $n = 8$.

5.4 FLUX METHOD FOR A RIVER CONFLUENCE

For the comparison of the analytical approach with the numerical one in case of a river confluence two values for the ratio of the width of the upstream polluted branch and the downstream river branch (B_1/B_s) are examined.

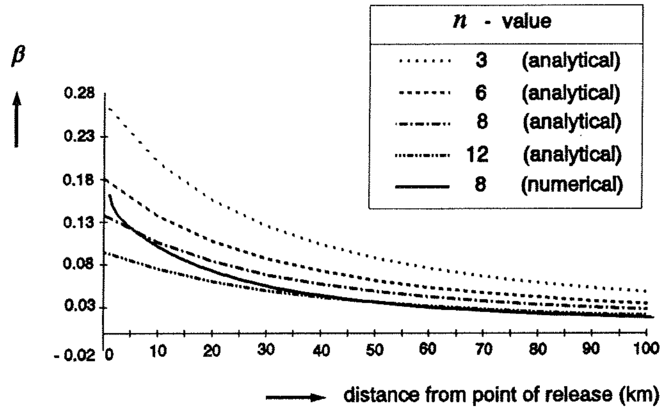

Fig. 21. Verification of the *flux method* with $B_1/B_s = 0.25$.

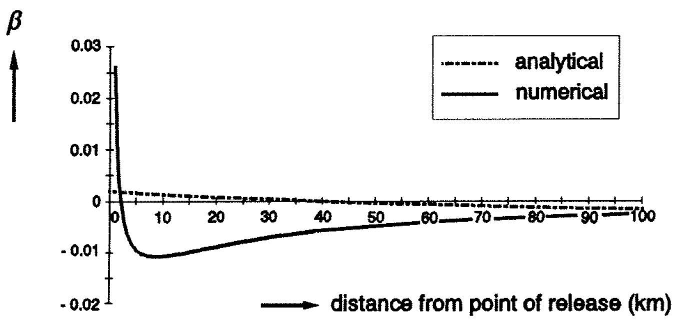

Fig. 22. Verification of the *flux method* with $B_1/B_s = 0.5$ and $\alpha = 0.23$.

The analytical computations are executed for several n-values (3 to 12) with a width ratio $B_1/B_s = 0.25$ (see Fig. 21). Near the point of release the lag coefficient after the numerical approach has a value of 0.13, which correspond with the analytical results for $n = 8$. At a distance of 20 km the n-value of 12 gives a better agreement with the numerically calculated lag-coefficients.

For a width ratio of $B_1/B_s = 0.50$ (Fig. 22) the numerically and analytically computed lag-coefficients are very small with values between -0.005 and 0.005. However, in case of the numerical approach an explicite decrease of the lag coefficient with the distance can be observed, while in case of the analytical computations the lag coefficient is already zero at the confluence, because the flow velocity and the velocity of the pollutant are equal.

Chapter 6

Numerical analysis of the River Rhine

6.1 GENERAL

For the analysis of the delay-coefficient in the River Rhine between the Lake of Constance and Basel the numerical model of the "Versuchsanstalt für Wasserbau (VAW)" (Hydraulic Research Institute) of the ETH-Zürich (Federal University of Technology of Zürich) is used.

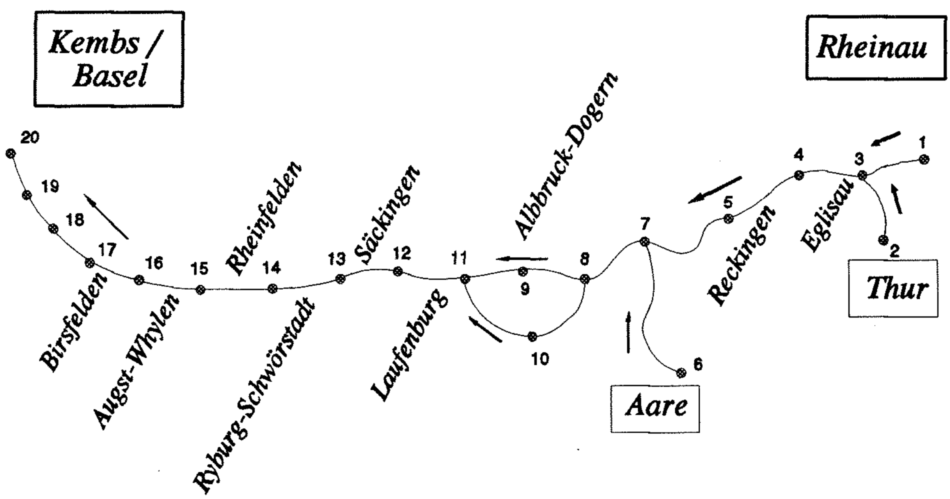

Fig. 23. Topography of the River Rhine between Lake of Constance and Basel.

The model describes the River Rhine from Rheinau (River-kilometre 58.83) till Kembs, downstream of Basel (River-kilometre 174).

The model includes also the following *power stations with weirs* (see also Fig. 23)

- Eglisau : 78.70 km
- Reckingen : 90.10 km
- Albbruck-Dogern : 112.75 km

- Laufenburg : 122.06 km
- Säckingen : 129.35 km
- Ryburg-Schwörstadt : 143.45 km
- Rheinfelden : 146.75 km
- Augst-Whylen : 155.85 km
- Birsfelden : 163.80 km

two *river confluences*:

- Rhine-Thur : 64.50 km
- Rhine-Aare : 102.50 km

and one *parallel channel* at the location of the power station Albbruck-Dogern from River-kilometre 109.00 till 113.50. In the model the river is represented by 12 branches and 155 cross sections.

The concerned pollutant consists of 200 kg of a conservative substance, released in 90 s. The point of release is located in the middle of the river at River-kilometre 58.83.

For the analysis of the behaviour of the lag coefficient the following aspects are taken into account:

* Water-level regulation caused by power stations;
* Distance over which the 'local' lag-coefficient is determined (see Eq.(19));
* Location of release;
* Discharge ratio AARE - RHINE in combination with the water-level regulation at power stations

and

* Differences between the "*mean*" and "*maximum*" lag coefficient. The "*mean*" lag-coefficient is based on the travel time of the centroid of the pollution cloud. The "*maximum*" lag-coefficient is based on the travel time of the maximum concentration of the cloud. For the calibration and verification of the lag coefficient in the 'Rhine Alarm Model' the maximum concentration of the measured concentration distributions of the tracer experiments was concerned.

6.2 WATER-LEVEL REGULATION BY WEIRS

As showed by the numerical results of an idealised river, the lag coefficient is heavily responding on discontinuities in the flow velocity, caused by weirs (see Section 4.3). Figure 24 shows that this influence on the lag coefficient is predominant. Each location of a peak of the delay-coefficient correspond with the location of a weir (i.e. water power station).

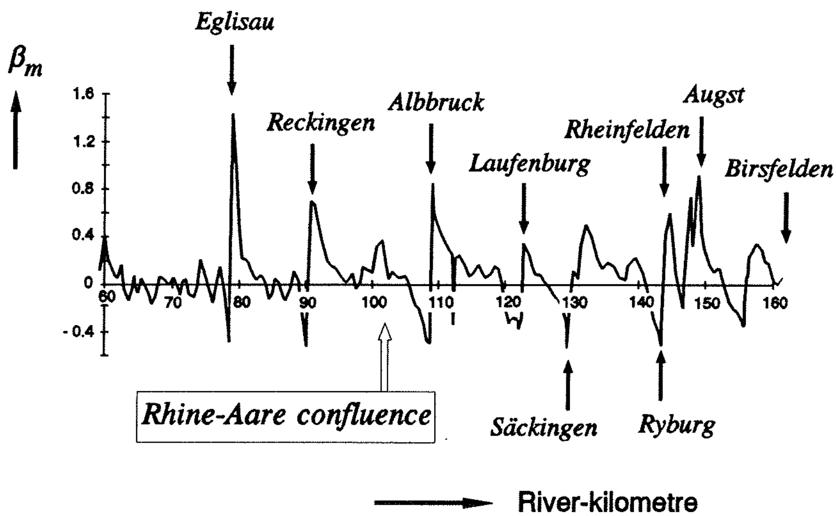

Fig. 24. Influence of the weirs as water-level regulators on the lag coefficient.

6.3 LOCAL LAG-COEFFICIENT AND THE DISTANCE CONCERNED

Another influence on the distribution of the lag coefficient along the river is the distance over which the 'local' lag-coefficient is determined. The reason for this influence comes from the definition of the lag coefficient (see Eq.(19)). The larger the distance, the larger the values for the travel times of the pollutant and flow become. This means that fluctuations of the lag coefficient can be reduced by taking larger distances. In other words without stagnant zones the lag coefficient tends to zero with the distance over which the local value is determined.

This means that the distinguished lengths of the reaches in which the River Rhine is schematized in the 'Rhine Alarm Model' influence the values of the lag coefficient. Moreover the locations at which the tracer measurements for the calibration of the lag coefficients were carried out, defines also the local values, because these locations normally do not coincide with the boundaries of the river reaches in the model.

Therefore a modification of the schematization of the River Rhine means a new calibration of the coefficient. Figures 25 and 26 give illustrations of these smoothing effects on the distribution of the lag coefficient. In Fig. 25 the distribution is presented for mean values over 15 cross sections after the River Rhine schematization of the model FLORIS. Figure 26 shows the distribution for the schematization after the 'Rhine Alarm Model'.

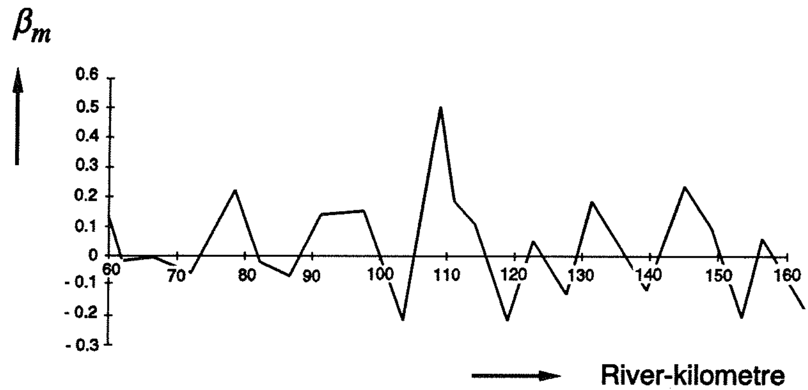

Fig. 25. Lag coefficients for each 15[the] FLORIS cross-section.

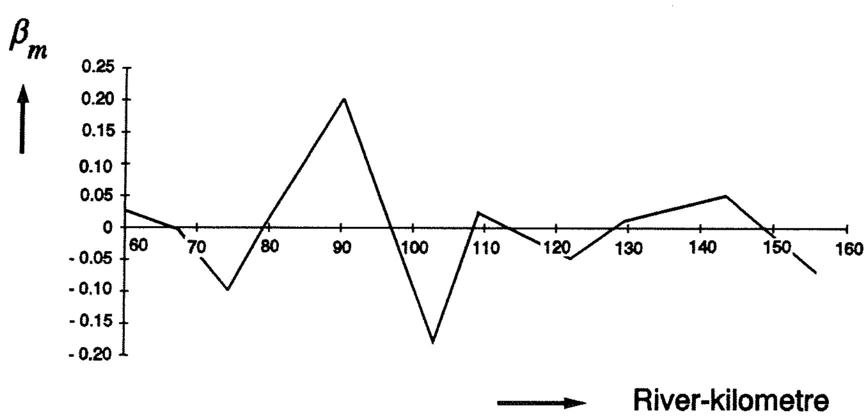

Fig. 26. Lag coefficients for each Rhine-Alarm-Model cross-section.

6.4 LOCATION OF RELEASE

In Fig. 27 the influence of the location of release of a pollutant on the lag coefficient is shown. As already discussed in Section 4.2 the different locations of the release gives a different behaviour of the lag coefficient. The small peaks in the distribution of the coefficient are caused by the water power stations.

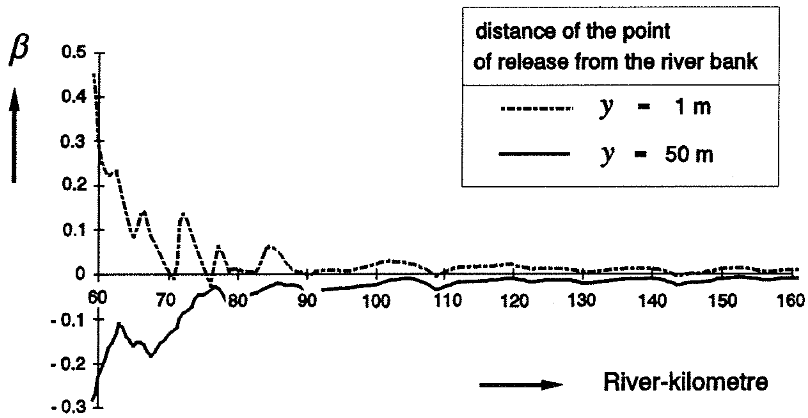

Fig. 27. Lag coefficients with different locations of release from the river bank.

6.5 DISCHARGE RATIO AARE - RHINE AND WATER-LEVEL REGULATION AT POWER STATIONS

The analysis of the influence of the discharge ratio AARE - RHINE on the delay-coefficient is carried out for the following situations (see also Fig. 28):

<u>*case a*</u> $Q_{rhine} = 490 \text{ m}^3/\text{s}$; $Q_{aare} = 550 \text{ m}^3/\text{s}$; ratio = 1.12

<u>*case b*</u> $Q_{rhine} = 930 \text{ m}^3/\text{s}$; $Q_{aare} = 1230 \text{ m}^3/\text{s}$; ratio = 1.32

<u>*case c*</u> $Q_{rhine} = 220 \text{ m}^3/\text{s}$; $Q_{aare} = 315 \text{ m}^3/\text{s}$; ratio = 1.43

The respective discharges concern the values upstream of the confluence. Because the water regulation at the power stations depends on the river discharge as well the influence of the discharge ratio AARE- RHINE also includes the effects of the power stations on the distribution of the lag coefficient. For comparison with the 'Rhine Alarm Model' the lag coefficients are determined per river reach after the 'Rhine Alarm Model'-schematization.

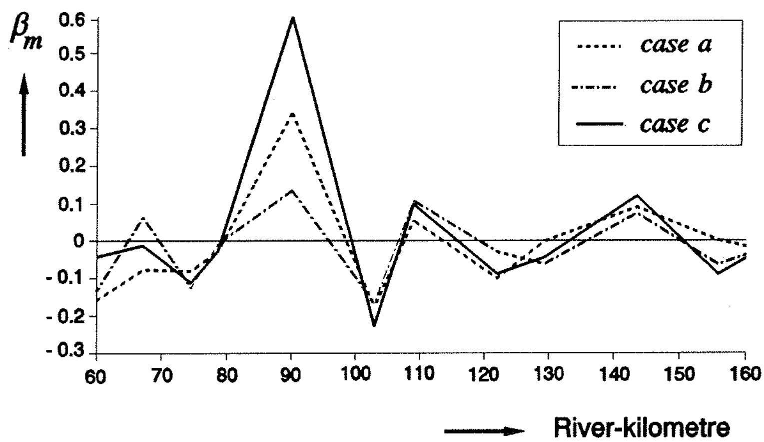

Fig. 28. Lag-coefficient distributions for different discharge ratios, according to the Rhine Alarm Model schematization.

Figure 28 shows the results for the three ratios. Upstream of the the confluence (River-kilometre 103) the lag coefficient has a relative large positive and downstream a relative large negative value.

Because downstream of the confluence at River-kilometre 112.75 the Albbruck-Dogern power station is situated, there are three phenomena to be distinguished resulting in a reduction of the velocity of the centroid of the pollution cloud upstream of the confluence:

(1) The backwater upstream of the confluence;

(2) The discontinuity of river width downstream of the confluence: the pollutant is transported with a smaller flow-velocity than the mean value (see Sub-section 4.3.3), which influences the velocity of the centroid of the cloud upstream of the confluence according to the turn-over process. This effect will be relatively small, because the discharges are of the same order of magnitude.

(3) The turn-over process related to the backwater effect upstream of the Albbruck-Dogern power station.

The discontinuity in the longitudinal profile of the flow velocity at the confluence should result in an increase of the velocity of the centroid of the cloud, corresponding with a negative value of the lag coefficient according to the turn-over process (see

Sub-section 4.3.2). The large positive values show that this effect is predominated by the reducing effects on the velocity of the centroid.

The negative value downstream of the confluence is caused by the turn-over process as a result of the discontinuity in the flow velocity at the Albbruck-Dogern power station as explained in Sub-section 4.3.2 (see also Fig. 15).

The positive value upstream of the confluence is maximal for the small river discharges and minimal for the large river discharges. The cause of this relation might be the dispersion. As a result of dispersion the longitudinal spreading of the cloud over a certain distance is less in case of large discharges than in the case of small discharges. Consequently the effects of the turn-over process is smaller in case of large discharges than in case of small discharges.

Other processes are difficult to estimate, because for instance the program PORIS did not encounter secondary streams.

6.6 MEAN-MAX LAG-COEFFICIENT

In the 'Rhine Alarm Model' the calibrated lag-coefficient is referred to the *maximum* of the measured concentration distributions instead of the centroid (i.e. the *mean* value of the concentration distribution).

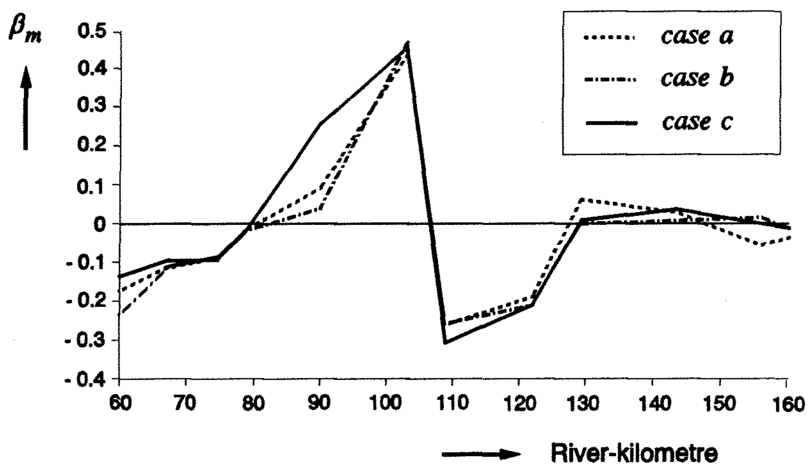

Fig. 29. Lag coefficients computed with the travel time referred to the maximum concentration.

The influence of this reference point of the concerned concentration distribution on the computation of the lag coefficient has to be faced, when the calculated lag coefficients has to be compared with the calibrated coefficients of the 'Rhine Alarm Model'.

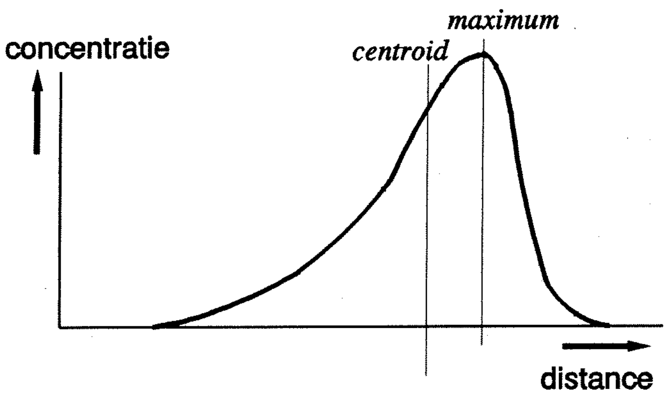

Fig. 30. Skewness of the concentration distribution.

Therefore the lag coefficient based on the travel time of the maximum of the concentration distributions is determined with the program PORIS for the three discharge ratios (a), (b) and (c), mentioned in the previous Sub-section. The results are presented in Fig. 29.

A comparison of the distribution of the '*maximum*' lag-coefficient with the '*mean*' value (Fig. 28) shows a great difference. Now the positive peak value is located downstream of the confluence (River-kilometre 103) and the negative value further downstream.

Because the concentration distribution is skew (Fig. 30) the maximum concentration is nearer to the front of the pollution cloud than the centroid. This means that the effect of the turn-over process is less than in case of the centroid (mean concentration) as reference point. The reduction of the velocity of the maximum concentration, resulting in a large positive value of the lag coefficient downstream of the confluence, is caused mainly by the backwater effect upstream of the Albbruck-Dogern power station and the discontinuity in the width downstream of the confluence. In case of a small river discharge (c) this effect influences also the lag coefficient upstream of the confluence as a result of the turn-over process in combination with a larger longitudinal spreading of the pollution cloud caused by the dispersion.
In succession the negative value of the lag coefficient occurs further downstream of the confluence.

Finally the hydrological situation during the tracer experiment "Rheinau - Basel" 1989 used for the calibration of the coefficients in the 'Rhine Alarm Model' is considered:

Q_{rhine} 550 m^3/s
Q_{aare} 490 m^3/s
location of release 58.8 km

In Fig. 31 the results of the computations with the program PORIS are compared with the calibrated values of the Rhine Alarm Model. The distribution of the calculated coefficient with PORIS is quite similar to the calibrated one. However, the values of the caulated coefficients are not completely equal. As well as for the negative as for the positive values the computed coefficients are (slightly) larger than the calibrated ones. An analysis in detail of these differences has not been carried out yet.

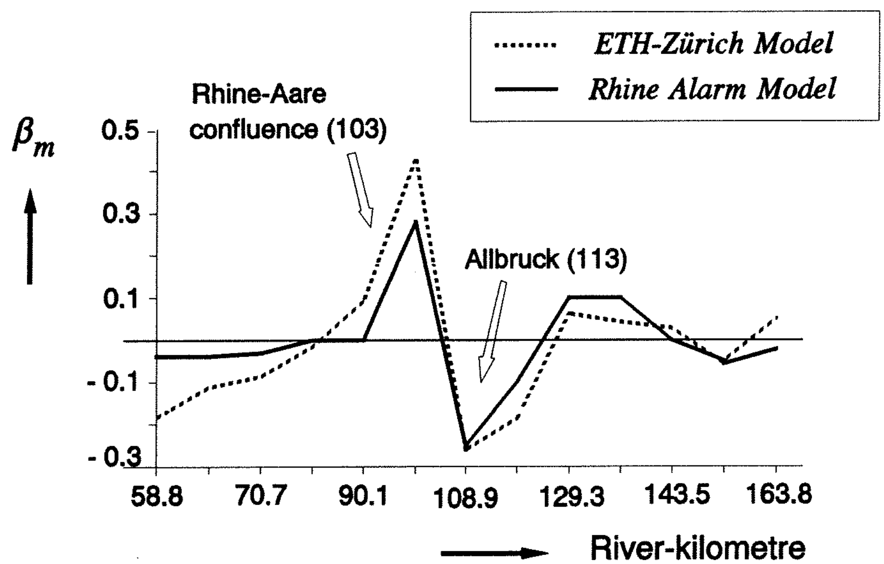

Fig. 31. Verification of the calibrated lag-coefficient of the Rhine Alarm Model.

Chapter 7

Conclusions and recommendations

There are three processes, influencing the lag coefficient:

(1) the two-dimensional effect caused by the transverse mixing;

(2) the two-dimensional effect caused by the transversal velocity-profile and the transversal spreading-width of the pollutant and

(3) the turn-over process: the velocity of the pollution cloud is determined by the longitudinal flow-velocity profile over the length of the cloud.

In case of a point releas at the river bank and a river confluence with one completely polluted river branch upstream of the confluence the two-dimensional aspects (1) and (2) are responsible for the influence on the coefficient as long as the pollutant is not completely mixed over the river cross-section.
In case of a confluence also the turn-over process (3) influences the lag coefficient. This influence is predominant for discharge ratios (ratio of the non-polluted river branch in relation to the polluted one) of the order of one or more with a discontinuity in the longitudinal flow-velocity profile.

As well as for a point release (at the river bank) as for a river confluence with a polluted branch upstream the analytical solutions for the 2-D convection-diffusion equation in combination with an exponential transversal velocity-profile give a good approximation of the longitudinal distribution of the lag coefficient.
If the river deals with irregularities of the cross-section geometry, the occurrences of weirs, etc. the analytical method does not give a sufficiently accurate approximation. In these cases numerical calculations have to be made.

In the Swiss part of the Upper-Rhine River the power stations with weirs for the water-level regulation cause discontinuities in the longitudinal flow-velocity profile. The effect of these discontinuities on the lag coefficient as a result of the turn-over process is predominant just upstream and downstream of the power stations. The delay-coefficient turns from a negative value upstream to a positive value downstream of the power station.

Further the value of the computed lag-coefficient depends on the length of the river reaches for which the relevant travel times are considered (see Eq.(19)). The larger the length concerned the more the value will be smoothed.

Because in the 'Rhine Alarm Model' the schematized river reaches of the Upper-Rhine River begin or end at a weir or confluence the effect of the turn-over proces on the lag-coefficient will be obvious and not smoothed down. As a matter of fact these locations are mostly chosen as measuring points of tracer experiments because of their accessibility. Therefore in case of tracer studies, especially in rivers with suppressed flow like the River Aare and the River Mosel, it is very important to be aware of the effects of the measuring location on the travel time of the tracer. Moreover, for the determination of the travel time of the tracer at locations in the vicinity of weirs or confluences it can make a difference if the travel time is related to the centroid or the maximum value of the measured concentration-distribution. Finally it has to be pointed out that the effect of the turn-over process is larger the more the tracer cloud is spread in the flow direction as a result of the dispersion.

The measured variations of the lag coefficient after the calibration experiment "Rheinau - Basel" 1989 could be explained by the two-dimensional aspects and the turn-over process, mentioned above. The results of the calculations with the two-dimensional transport model PORIS of the Hydraulic Research Institute (VAW) of the Federal University of Technology of Zürich (ETH-Zürich) confirm the calibrated values of the 'Rhine Alarm Model'.
However, the model PORIS does not describe secondary flow. Thus the influence of these flow patterns on the lag coefficient could not be analysed.

Main Symbols

B_1	width upstream of a confluence	[L]
B_s	width of the river	[L]
c	pollution cloud velocity	[L/T]
a	water depth	[L]
K_y	transversal mixing coefficient	[L^2/T]
L_m	mixing length	[L]
M	total mass of release	[M]
n	exponential constant of the flow-velocity profile	[-]
Q	river discharge	[L^3/T]
Q_1	discharge of the polluted branch upstream of the confluence	[L^3/T]
Q_2	discharge of the non-polluted branch upstream of the confluence	[L^3/T]
T_{flow}	travel time based on the flow velocity	[T]
T_{pol}	travel time of the pollution cloud	[T]
$u(y)$	flow velocity	[L/T]
u_s	mean flow-velocity at a cross-section	[L/T]
u_1	flow velocity in the polluted branch upstream of the confluence	[L/T]
u_2	flow velocity in the non-polluted branch upstream of the confluence	[L/T]
u_*	shear velocity	[L/T]
x	x-coordinate (flow direction)	[L]
x'	dimensionless distance from the point of release	[-]
$x_{centroid}$	x-coordinate of the centroid of the pollution cloud	[L]
x_{inlet}	x-coordinate of the point of release	[L]
X_1	dimensionless distance from a bank release (flow direction)	[-]
y	y-coordinate (perpendicular to the flow direction)	[L]
y'	dimensionless distance from a river bank	[-]
y_1	pollution width	[L]
α	constant of proportionality	[-]
β	overall lag-coefficient	[-]
β_m	local lag-coefficient	[-]
φ_0	1-D concentration	[M/L^3]
$\varphi(x,y)$	2-D concentration	[M/L^3]

References

ABRAMOWITZ, M. and STEGUN, I.A. (1965)
Handbook of mathematical functions, Dover Public. Inc., New York

CHATWIN, P.C. and ALLEN, C.M. (1985)
Mathematical Models of dispersion in rivers and estuaries,
Annual Rev. Fluid Mechanics, vol. **17** 119-149

DENTON, R. A. (1990)
Analytical asymptotic solutions for longitudinal dispersion with dead zones, *Journal of Hydraulic Research*, vol. **28**, no. 28, pp. 309...329

FISCHER H.B., E.J.LIST, R.C.Y.KOH, J.IMBERGER and N.H.BROOKS (1979)
Mixing in Inland and Coastal Waters, Academic Press, New York, London

LEIDBUNDGUT Ch. (1988)
Markierversuch Rhein 'Allbruck-Basel', Geographisches Institut Bern

LEIDBUNDGUT Ch. (1989)
Markierversuch Rhein 'Rheinau-Basel', Geographisches Institut Bern

HOLLEY, Forrest M. (1983)
Field calibration of stream-tube dispersion Model,
Journal Hydr. Eng., Vol. **109**, no. 11, Nov 1983, 1455...1470

MAZIJK, A. van (1992)
Neukalibrierung und Verifikation der Hochrheinstrecke im Rheinalarmmodell Version 2.1, TU Delft, Juni 1992

NOPPENEY, R.M. (1988)
Gevoeligheidsonderzoek Alarmmodel Rijn, TU Delft, Nov. 1988

NORDIN, C.F. and TROUTMAN, B.M. (1988)
Longitudinal Dispersion in rivers: the persistence of skewness in observed data, *Wat. Resour. Res.*, Vol. **16**, 123...128

PURNAMA, A. (1988)
The effect of deadzones on longitudinal dispersion in streams, *Journal fluid mechanics*, vol. **186**, 351...377

REICHERT P. and WANNER. O (1991)
Enhanced One-Dimensional Modeling of transport in Rivers, *Journal of hydraulic engineering*, vol. **117**, no. 9, pp. 1165...1183, sept. 1991

TAYLOR, G.I. (1954)
The dispersion of matter in turbulent flow through a pipe, *Proc. R. Society London Ser.*

VAW (1991)
FLORIS, ein hydrodynamisches Modell zur Simulation instationärer Abflüsse in offenen Gerinnen, Zürich

VAW (1991)
Benutzershandbuch FLORIS

VAW (1990)
Fließzeiten im Rhein. Berechnung von mittlereren Abflußgschwindigkeiten und Fließzeiten mit dem hydrodynamischen Modell FLORIS

VAW (1991)
Stofftransportmodelle für Fließgewässer, Zwischenbericht, Zürich, Dezember 1991
VRIES, M. de (1984)
Vloeistofmechanica, TU Delft Civiele Techniek
YOTSUKURA, N. and SAYRE, W. (1976)
Transverse mixing in natural rivers, *Water Resources Research* vol. **12**, no. 4, 695...704, aug. 1976

Appendix

Linear spreading method

In rivers the release of a pollutant mostly takes place at the river bank. In these cases there are three mixing phases to be distinguished:

- a first phase in which vertical mixing is predominant;
- the second phase in which transversal mixing over the cross-sectional area of the river is predominant and
- the third phase in which longitudinal mixing is predominant for the distribution of the concentration of the released substance.

The distance over which vertical mixing has become complete, is relative short (about 60 till 100 times the waterdepth, Fischer, 1979). In such situations the transport of soluble conservative substances in rivers can be mostly described in terms of concentration (φ) as a function of time (t) and place (x,y) by the convection-dispersion equation, according to Taylor (1954)

$$\frac{\partial \varphi}{\partial t} + u_s \frac{\partial \varphi}{\partial x} - K_x \frac{\partial^2 \varphi}{\partial x^2} - K_y \frac{\partial^2 \varphi}{\partial y^2} = 0 \qquad \text{(A.1)}$$

if the longitudinal and transversal dispersion-coefficients K_x and K_y are independent of x and y respectively, while u_s is the mean flow-velocity.

For the determination of the distance over which completely mixed situation over the cross-section is achieved, a constant release of a conservative substance W is considered. Neglecting the longitudinal dispersive transport compared to the transversal one, the following solution of Eq.(A.1) is found

$$\frac{\varphi(x,y)}{\varphi_0} = \frac{1}{\sqrt{(\pi K_y x)/(u_s \cdot B_s^2)}} \cdot \sum_{n=-\infty}^{n=\infty} \left(\exp \left(- \frac{(y/B_s - 2n)^2}{(4K_y x)/(u_s \cdot B_s^2)} \right) \right) \qquad \text{(A.2)}$$

with

φ_0 average cross-sectional concentration (W/A)
A cross-sectional area of the river
B_s width of the river

Introducing the dimensionless parameters for

the concentration	$\varphi\,(x',y')\,/\,\varphi_0$
the longitudinal distance	$x' = x \cdot K_y\,/\,[u_s \cdot B_s^2]$
the tranversal distance	$y' = y\,/\,B_s$

Eq.(A2) can be rewritten into

$$\frac{\varphi\ (x',y')}{\varphi_0} = \frac{1}{\sqrt{\pi \cdot x'}} \sum_{n=-\infty}^{\infty} \left[\exp\left(- \frac{(y' - 2n)^2}{4x'} \right) \right] \qquad (A.3)$$

In Fig. A.1 the dimensionless concentration $\varphi(x',y')/\varphi_0$ is presented as a function of the dimensionless distance x' for some dimensionless positions in the cross section y'.

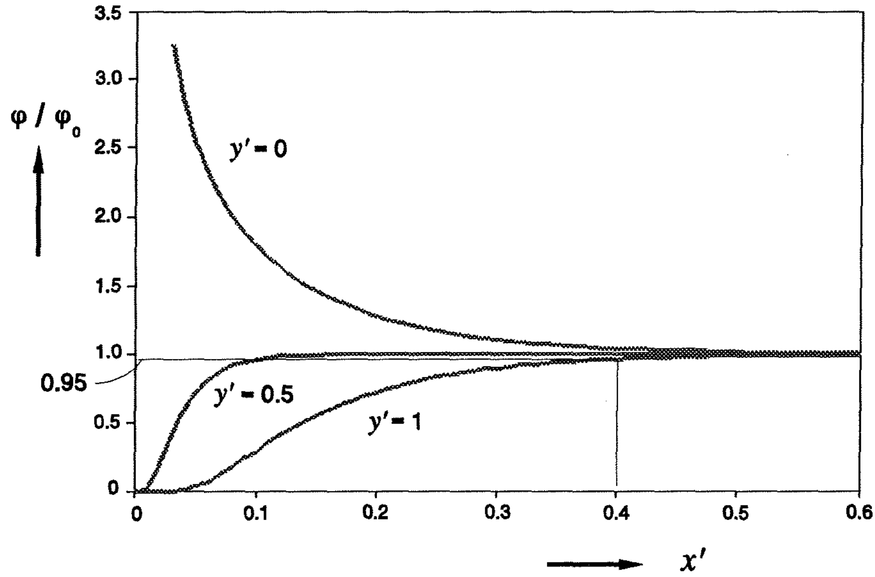

Fig. A.1. Distribution of φ/φ_0 asa function of x' and y' (constant release of a conservative substance at $y' = 0$).

If the completely mixed situation is defined by $\varphi(x',y')/\varphi_0 \geq 0.95$ for $y' = 1$, then the "mixing length" $x = L_m$ can be derived from Fig. A.1, being the distance over which the released substance is "completely mixed" over the cross-section. Because the corresponding dimensionless $x' = 0.4$, the "mixing length" becomes

$$L_m \approx 0.4 \cdot \frac{u_s \cdot B_s^2}{K_y} \qquad (A.4)$$

In the second phase (transversal mixing) the transport velocity c will be less than the mean flow velocity u_s due to the velocity distribution over the cross-sectional area of the river (Fig. A.2).

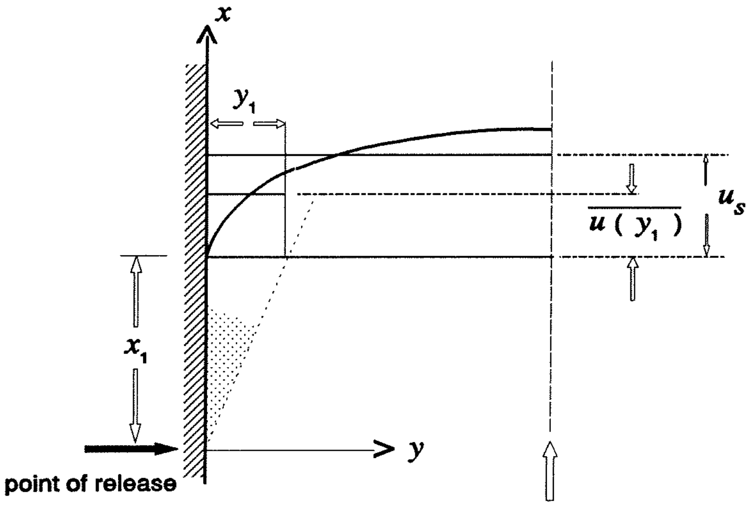

Fig. A.2. Average velocity over the width of the plume of the released substances.

In order to formulate a relation between these two velocities, the velocity distribution over the width of the river (depth averaged) is supposed to be symmetrical to the centre of the river and is defined by (for $0 \leq y \leq 0.5\,B_s$)

$$u(y) = \frac{n+1}{n} \cdot \left(\frac{y}{0.5 B_s} \right)^{1/n} \cdot u_s \qquad \text{(A.5)}$$

wherein n stands for a constant between 3 and 10, depending on the distribution of the velocity profile in relation to the wall roughness (Fig. A.3).

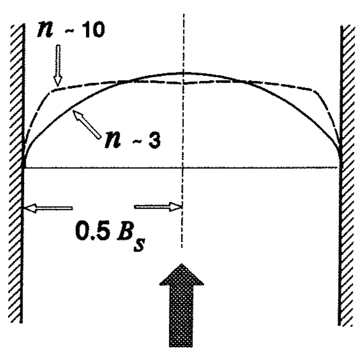

Fig. A.3. Velocity profiles in relation to the n-value.

By integration of Eq.(A.5) the average value of the flow velocity over the distance y from 0 to y_1 ($y_1 \leq 0.5\,B_s$) is found

$$\overline{u(y_1)} = \left(\frac{2}{B_s} \cdot y_1 \right)^{1/n} \cdot u_s \qquad \text{(A.6)}$$

Assuming a linear transversal spreading of the pollutant with the distance to the point of release and a completely mixed situation over the distance y_1 (see also Fig. 5), the transport velocity at a certain distance x_1 is determined by the flow velocity $\overline{u(y_1)}$ with (Fig. A.2)

$$y_1 = \frac{x_1}{L_m} \cdot B_s \tag{A.7}$$

thus Eq.(A.6) becomes

$$c(x) = \overline{u(y_1)} = \left(\frac{2}{L_m} \cdot x\right)^{1/n} \cdot u_s \tag{A.8}$$

and with the dimensionless distance $X = x/L_m$

$$c(X) = (2 \cdot X)^{1/n} \cdot u_s \tag{A.9}$$

Substitution of Eq.(A.9) into the expression for the lag-coefficient β

$$\beta = \frac{u_s}{c} - 1 \tag{A.10}$$

gives

$$\beta(X) = (2 \cdot X)^{-1/n} - 1 \tag{A.11}$$

being the local value of β of at a distance X from the point of release.

The overall value of the lag coefficient between the point of release and $X = X_1 \leq 0.5$ is found by integration of Eq.(A.11)

$$\begin{aligned} \overline{\beta(X_1)} &= \frac{1}{X_1} \int_0^{X_1} \left[(2 \cdot X)^{-1/n} - 1 \right] dX \\ &= \frac{n}{n-1} \cdot (2 \cdot X_1)^{-1/n} - 1 \end{aligned} \tag{A.12}$$

For values of $B_s \geq y_1 > 0.5\, B_s$ the average flow-velocity becomes with $y_1 = B_s - y_1'$, while y_1' is the distance from the opposite river-bank.

$$\overline{u(y_1)} = \frac{n+1}{n} \cdot u_s \cdot \frac{1}{y_1} \cdot \left[2 \cdot \int_0^{0.5 \cdot B_s} \left(\frac{y}{0.5 B_s} \right)^{1/n} dy - \int_0^{y'_1} \left(\frac{y}{0.5 B_s} \right)^{1/n} dy \right] \tag{A.13}$$

which gives in succession

$$\overline{u(y_1)} = \frac{n+1}{n} \cdot u_s \cdot \frac{1}{y_1} \cdot \left[\left(\frac{n}{n+1} \cdot B_s \right) - \left((0.5 B_s)^{-1/n} \cdot \frac{n}{n+1} \cdot \left(y'_1\right)^{\frac{n+1}{n}} \right) \right]$$

(A.14)

$$\overline{u(y_1)} = u_s \cdot \frac{1}{y_1} \cdot \left[B_s - \left((0.5 B_s)^{-1/n} \cdot \left(y'_1\right)^{\frac{n+1}{n}} \right) \right]$$

$$\overline{u(y_1)} = u_s \cdot \frac{B_s}{y_1} \cdot \left[1 - 2^{1/n} \cdot \left(\frac{y'_1}{B_s} \right)^{\frac{n+1}{n}} \right]$$

$$\overline{u(y_1)} = u_s \cdot \frac{B_s}{y_1} \cdot \left[1 - 2^{1/n} \cdot \left(\frac{B_s - y_1}{B_s} \right)^{\frac{n+1}{n}} \right] \qquad \text{(A.15)}$$

Substitution of Eq.(A.7)

$$y_1 = \frac{x}{L_m} \cdot B_s = X \cdot B_s \qquad \text{(A.7)}$$

into Eq.(A.15) gives

$$\overline{u(y_1)} = c(X) = u_s \cdot \frac{1}{X} \cdot \left[1 - 2^{1/n} \cdot (1 - X)^{\frac{n+1}{n}} \right] \qquad \text{(A.16)}$$

Applying Eq.(A.10), it yields

$$\beta(X) = \frac{X}{1 - 2^{1/n} \cdot (1 - X)^{(n+1)/n}} - 1 \qquad \text{(A.17)}$$

The overall value of the lag coefficient for $1 \geq X_1 > 0.5$ is found by integration of Eqs (A.11) and (A.17)

$$\overline{\beta(X_1)} = \frac{\int_0^{0.5} \left[(2 \cdot X)^{-1/n} - 1 \right] \mathrm{d}X + \int_{0.5}^{X_1} \left[\frac{X}{1 - 2^{1/n} \cdot (1 - X)^{(n+1)/n}} - 1 \right] \mathrm{d}X}{X_1}$$

(A.18)

Because the second term at the right part of Eq.(A.18) can not be solved analytically, it is done numerically with steps $\Delta X = 0.01$.

$$\overline{\beta(X_1)} = \frac{1}{X_1} \left(\left[\frac{0.5}{n-1} \right] + \int_{0.5}^{X_1} \left[\frac{X}{1 - 2^{1/n} \cdot (1 - X)^{(n+1)/n}} - 1 \right] \mathrm{d}X \right)$$

(A.19)

In Fig. A.4 the expression for $\overline{\beta(X_1)}$ according to Eqs (A.12) and (A.19), is presented graphically.

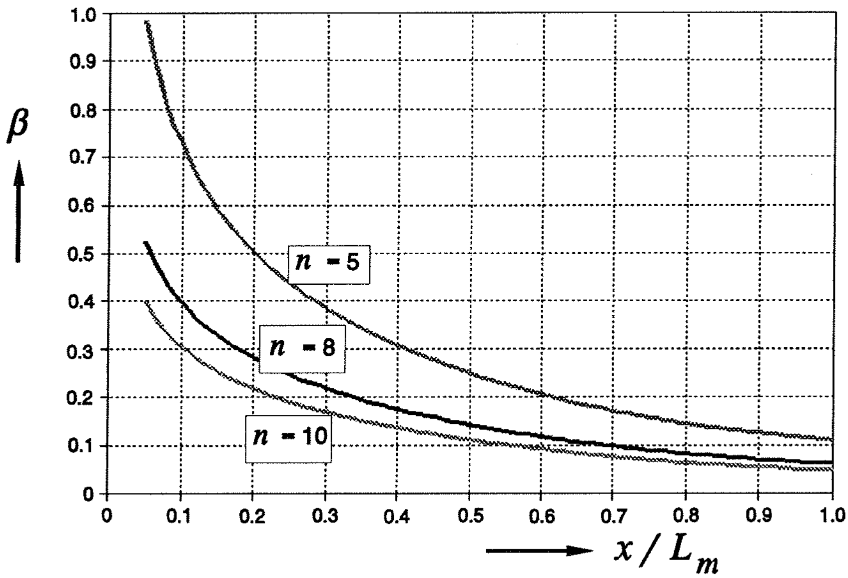

Fig. A.4. Effect of the velocity distribution on the transport velocity.